JTTEE5 15:131-140
DOI: 10.1361/105996306X92695
1059-9630/$19.00 © ASM International

Nickel-Chromium Plasma Spray Coatings: A Way to Enhance Degradation Resistance of Boiler Tube Steels in Boiler Environment

Buta Singh Sidhu and S. Prakash

(Submitted February 17, 2005; in revised form July 14, 2005)

Boiler tube steels, namely low carbon steel ASTM-SA210-Grade A1 (GrA1), 1Cr-0.5Mo steel ASTM-SA213-T-11 (T11), and 2.25Cr-1Mo steel ASTM-SA213-T-22(T22), were used as substrate steels. Ni-22Cr-10Al-1Y powder was sprayed as a bond coat 150 μm thick before a 200 μm final coating of Ni-20Cr was applied. Coatings were characterized prior to testing in the environment of a coal fire boiler. The uncoated and coated steels were inserted in the platen superheater zone of a coal fired boiler at around 755 °C for 10 cycles, each 100 h. Coated steels showed lower degradation (erosion-corrosion) rate than uncoated steels showed. The lowest rate was observed in the case of Ni-20Cr coated T11 steel. Among the uncoated steels, the observed rate of degradation was the lowest for the T22 steel.

Keywords coatings, coal fired boilers, degradation, Ni-20Cr, plasma spray

1. Introduction

Coal gasification systems operate up to 1093 °C and at a pressure of up to 10 MPa, depending on the specific process and the product. In addition to hydrogen and carbon-containing gaseous species, there are many undesirable species including sulphides, sulphites, sulphates, ammonia, cyanides, volatilized oils, phenols, and aggressive trace elements such as potassium, sodium, vanadium, and lead (Ref 1). The corrosive nature of this gaseous environment may cause rapid material degradation and result in premature failure of components (Ref 2, 3).

Surface degradation of metal containment walls and heat exchanger tubing by a combined erosion-corrosion (E-C) mechanism have been experienced in some boilers, particularly fluidized bed combustors (Ref 4). It was observed primarily that E-C occurred as a single phenomenon that integrated both chemical and mechanical behavior of the base metal and the boiler gas particles. It was further predicted that the loss of sound metal is related to the rate of oxidation.

Prakash et al. (5) have studied the boiler tube failure in coal fired boilers. A case study covering one year has been conducted and it was observed that more than 50% of the failures were attributed to the hot corrosion and erosion due to ash. Although corrosion problems cannot be completely remedied, it is estimated that corrosion-related costs can be reduced by more than 30% with development and use of better corrosion control technologies. Corrosion control measures include corrosion inhibitors, cathodic protection, and coatings (Ref 6).

The demand for protective coatings has increased recently for almost all types of superalloys with improved strength, since high-temperature corrosion problems become much more significant for these alloys with increasing operating temperatures of modern heat engines. Plasma techniques have many advantages such as a high productivity for producing coatings of more than 100 μm. Furthermore, the process does not degrade the mechanical properties of the substrate (Ref 7).

Plasma spraying has been successful as a reliable cost-effective solution for many industrial problems (Ref 8). Coatings have been used in areas of liquid and high-temperature corrosion and wear protection and also in special applications for thermal, electrical, and biomedical purposes (Ref 9).

The prime advantage of the plasma spray technique is that it enables a whole range of materials, including metals and alloys, to be coated on to a great variety of substrate types and geometries (Ref 10, 11).

Erosion wear and mechanical properties of nickel- and iron-based as well as chromium-nickel plasma sprayed coatings on carbon steel have been studied by Hidalgo et al. (Ref 12, 13) in the simulated industrial service conditions of boilers. These types of coatings are used on heat transfer and structural elements in boilers. The use of plasma sprayed Ni-Cr coatings on stainless steel surfaces to protect them from the high temperature and erosive conditions encountered in power plant boilers has been further reported by Hidalgo et al. (Ref 14).

The present investigation aims to evaluate the degradation resistance of Ni-20Cr plasma sprayed boiler tube steels in industrial environments. The samples were tested in the platen superheater zone of a coal fired boiler for a 1000 h exposure period. The degradation rate was evaluated in terms of metal thickness lost. Techniques of x-ray diffraction (XRD), scanning electron microscopy (SEM)/energy dispersive x-ray (EDAX), and electron probe microanalysis (EPMA) were used to analyze the corroded products.

Buta Singh Sidhu, Department of Mechanical Engineering GZS, College of Engineering and Technology Bathinda (Punjab)-151001, India; and **S. Prakash,** Department of Metallurgical and Materials Engineering, Indian Institute of Technology, Roorkee-247667 India. Contact e-mail: butasidhu@yahoo.com.

2. Technical Procedure

2.1 Development of Coatings

The three types of substrate steel were used: low carbon steel ASTM-SA210-Grade A1 (GrA1), 1Cr-0.5Mo steel ASTM-SA213-T-11 (T11), and 2.25Cr-1Mo steel ASTM-SA213-T-22(T22). Samples were grit blasted before plasma spraying. A 40 kW Miller thermal plasma spray system available from Anod Plasma Spray Ltd. (Kanpur, India) was used to apply the coatings. Ni-20Cr-10Al-1Y powder was used for producing a bond coat of approximately 150 μm thick before applying the final coatings of Ni-20Cr (200 μm). The detailed procedure of coating along with the composition of the base steels and alloy powder was reported elsewhere (Ref 14-18).

2.2 Industrial Environment Studies

The samples were tested in the middle zone of a platen superheater of the Stage-III Boiler of Guru Nanak Dev Thermal Plant (Bathinda, Punjab, India). The samples were hung using a stainless steel wire passed through a 1 mm hole drilled in the samples. They were hung through the soot blower dummy points at a height of 31.5 m from the base of the boiler. The average temperature was about 755 °C with a variation of ±10 °C. The average volumetric flow of flue gases was 231 m^3/s. The SO_x and NO_x values of the flue gases were 236 and 1004 $\mu g/m^3$, respectively. The analysis of flue gases showed the presence of 12% CO_2 and 7% O_2.

The samples were exposed to the combustion gases for a total of 10 cycles, each consisting of a 100 h exposure followed by 1 h cooling at ambient conditions. After each cycle, the samples were visually inspected for any surface change, and the samples weights were measured subsequently. At the end of the cyclic study, the samples were characterized using XRD, SEM, EDAX, and EPMA, and the measurement of scale thickness was also performed.

Because of suspected spalling and ash deposition on the samples, the weight change data could not be used directly for predicting degradation behavior. Further, the weight change data were also affected by the corrosion caused by the ash. In view of these facts, the extent of degradation was monitored by measuring the thickness of the unreacted samples after the total exposure of 1000 h. From the thickness loss data, the degradation (E-C) rates in millimeters per year were evaluated.

3. Results

3.1 Coating Characterization

3.1.1 Coating Thickness and Porosity Measurements. The back scattered electron image (BSEI) for Ni-20Cr coated steel is shown in Fig. 1. The inner coated layer is the bond coat, i.e., NiCrAlY and the outer layer is Ni-20Cr coating. The coatings thicknesses were measured from these BSEI micrographs and are compiled in Table 1.

The coatings porosity is of prime importance in the hot corrosion studies. Dense coatings would provide good corrosion resistance compared with porous coatings. The average porosity of the coatings was found to be 3.1%.

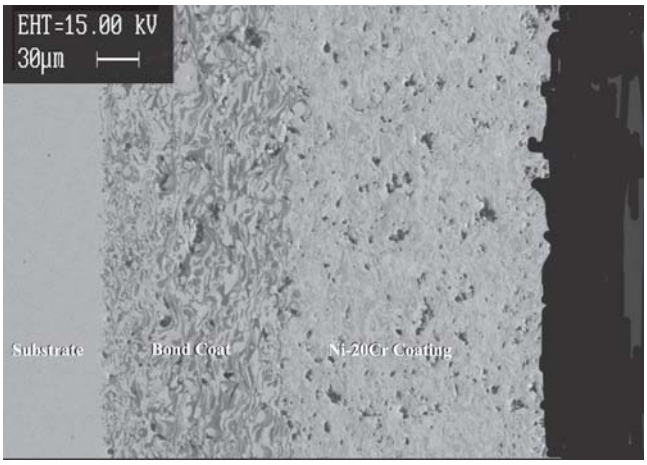

Fig. 1 SEM micrographs showing cross-section morphologies of Ni-20Cr coating on GrA1 steel

Table 1 Coating thickness and porosity for Ni-20Cr coating

Type of coating	Coating thickness, μm: Bond coat NiCrAlY	Outer coat	Total	Average porosity, %
Ni-20Cr	152	213	365	3.1

3.1.2 Microhardness Measurements. Microhardness profiles versus distance from the coating-substrate interface are given in Fig. 2. The critical hardness values of the substrate steels were found to be in the range 200-300 Hv. The maximum measured microhardness of the Ni-20Cr coating was about 900 Hv.

3.1.3 SEM/EDAX Analysis. The SEM micrograph shown in Fig. 3 indicates melting, and these phases are accompanied by precipitates along them. Two phases are present: one is nickel-rich and the other contains more amount of chromium.

3.2 Degradation Behavior

The coating degradation for uncoated and Ni-20Cr coated steels expressed in weight change per unit area (mg/cm^2) has been plotted as a function of time in Fig. 4. Due to severe spalling, GrA1 steel exhibited a decrease in weight change values. The weight gain values after 1000 h for the T22 steel is around 2/3 of the weight gain value of the T11 steel and has also shown lesser spalling tendency. The minimum weight change was observed for the coated GrA1 steel and is about 2/3 that for Ni-20Cr coated T11 steel. The weight gain values of the coated T11 and T22 steels are almost identical.

The extent of degradation in terms of metal thickness lost and E-C rates in mm/year are reported in Table 2. Ni-20Cr coated T11 steel has shown a minimum loss of metal thickness that was about 2/3 of that for the uncoated T11 steel.

3.3 Surface Analysis

The SEM micrograph shown in Fig. 5(a) for the corroded surface of the uncoated T22 steel exposed to boiler conditions

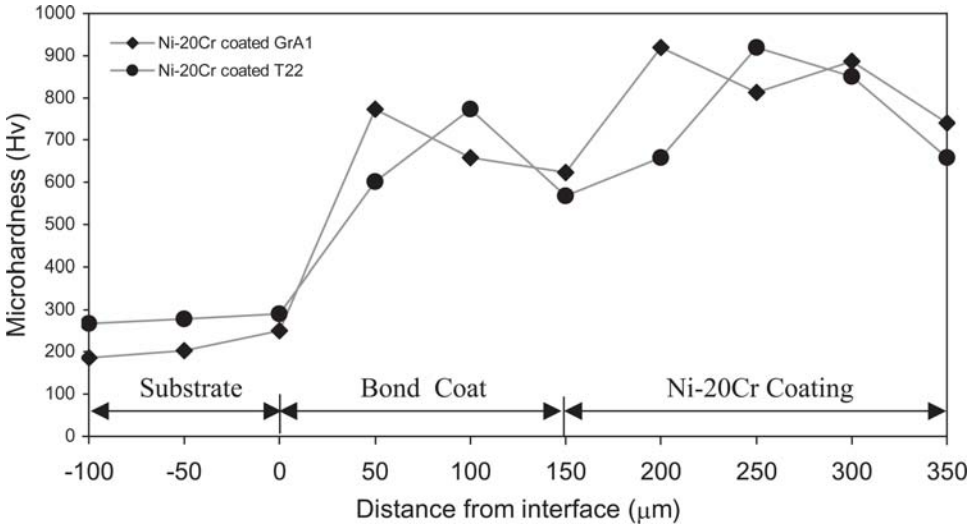

Fig. 2 Cross-sectional microhardness profiles of Ni-20Cr coating for different base steels with bond coat of NiCrAlY

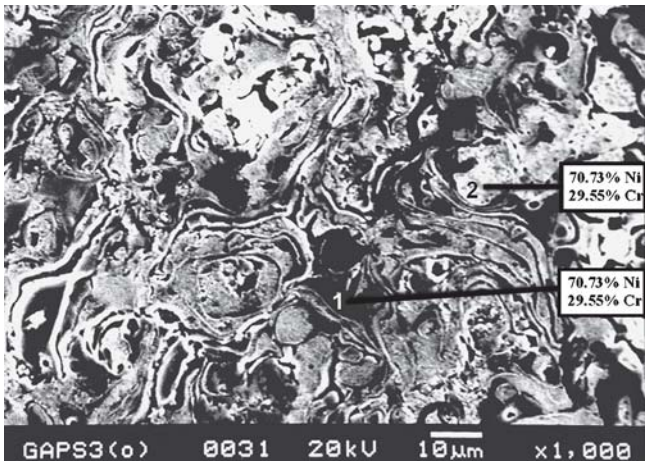

Fig. 3 SEM/EDAX analysis of Ni-20Cr coatings showing elemental composition (wt.%) at various points

indicates a continuous granular scale consisting mainly of Fe_2O_3 (91.84) and some amounts of SiO_2 (5%) and Al_2O_3 (2%) (point 2 in the micrograph). Some ash particles can be seen embedded in the scale as white color nodules. These consist of 40% Al_2O_3, 53% SiO_2, and 7% Fe_2O_3 (point 1 in the micrograph). The SEM micrograph shown in Fig. 5(b) for the Ni-20Cr coated T22 steel indicated the presence of a main scale of NiO with alumina and silica. The presence of Al_2O_3 (18.7%), SiO_2 (22.8%), and Fe_2O_3 (54.8%) as revealed by the EDAX analysis at point 2 in the micrograph may be attributed to the ash embedment into the scale. Spalled areas are rich in nickel with some amount of alumina and silica.

The x-ray diffractograms for GrA1, T11, and T22 base steels after exposure to a boiler environment for 1000 h are shown in Fig. 6. In the given environment, all the steels have Fe_2O_3 as the main constituent of scale. In addition to Fe_2O_3, the diffractograms indicated the presence of Al_2O_3. The XRD pattern of the scales of the coated steels after exposure to coal fired boiler environment shows similar phases, as shown in Fig. 7. The main phases revealed by XRD analysis are NiO, Cr_2O_3, $NiCr_2O_4$, Al_2O_3, and Fe_2O_3.

3.4 Cross-Sectional Analysis

3.4.1 EDAX Analysis. Cross-section oxide scale morphology and elemental composition for substrate steels T11 and T22 after 1000 h exposure to hot flue gases of coal fired boiler are shown in Fig. 8. The SEM micrographs show thick scale mainly consisting of iron oxide for both steels after 1000 h exposure, as shown by the elemental composition profiles. The outer thin layer of the scale of the T11 steel contains silicon; whereas for the T22 steel, this layer has a higher percentage of silicon greater than 3% at point 3. The scale of the T22 steel is comparatively thicker than the scale on T11 steel, Fig. 8(b). Both boiler steels have revealed the presence of chromium in the subscale, where it is up to 3% for the T22 steel. For T22 boiler steel, Mo is also present along with Cr.

Scale morphology and EDAX analysis for the corroded cross section of Ni-20Cr coated T11 and T22 steels after 1000 h exposure is shown in Fig. 9. Both steels have shown almost identical elemental variations across the specimens. However, the scale of the T11 steel spalled from the substrate. Iron has remained confined in the substrate whereas nickel diffused into the substrate. The bond coat has retained its identity by forming oxides of nickel, aluminium, chromium, and yttrium. The outer part of the scale consists mainly of oxides of nickel and chromium. This is an indication of oxygen penetration into the steel substrates.

3.4.2 EPMA Analysis. BSEI and elemental x-ray maps obtained for the spalled scale piece of the GrA1 boiler steel exposed to the boiler environment for 1000 h are shown in Fig. 10. The scale mainly contains iron, which indicates the formation of Fe_2O_3. Coexistence of aluminium and silicon reveals the embedment of ash particles in the scale.

From the composition images shown in Fig. 11 for the Ni-20Cr coated GrA1 steel after exposure, the bond coat can be clearly identified. The top scale consists of nickel and chromium. At the scale substrate interface, there is a chromium-rich

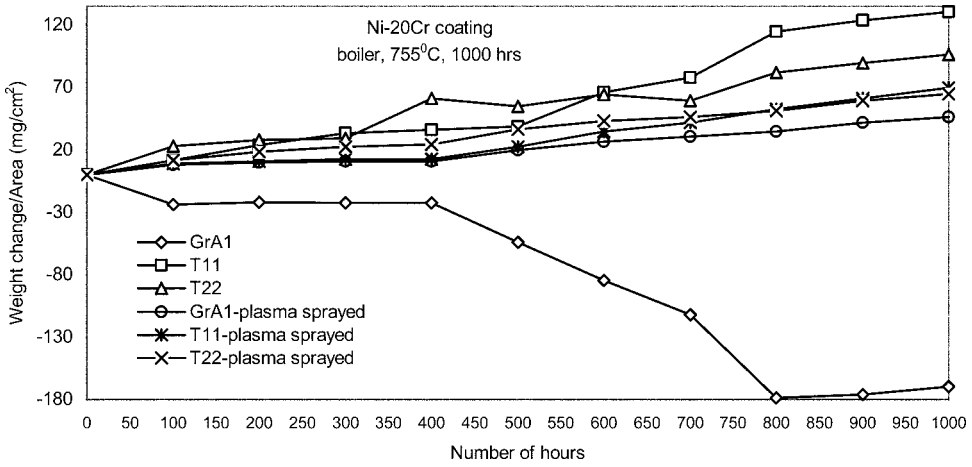

Fig. 4 Weight change profile for uncoated and Ni-20Cr coated steels with bond coat exposed to platen superheater of the coal fired boiler for 1000 h at 755 °C

Table 2 Metal thickness lost and erosion-corrosion rates for uncoated and Ni-20Cr plasma sprayed steels
After 1000 h of exposure to platen superheater of the coal fired boiler at aroud 755 °C

	Metal thickness lost, mm			Degradation rate, mm/year		
Type of steel	**GrA1**	**T11**	**T22**	**GrA1**	**T11**	**T22**
Uncoated	1.096	1.073	0.99	9.606	9.402	8.472
Ni-20Cr coated	0.703	0.685	0.796	6.156	6.005	6.979

thin layer, and above this, sulphur is present. Silicon, aluminium, and iron coexist at the top of the scale. The lower part of the bond coat is rich in nickel. From the bond coat, nickel and chromium have diffused outward to form the scale. EPMA line profile analysis presented in Fig. 12 for this coated steel indicates that the oxygen has penetrated through the Ni-20Cr coating to the bond coat and formed the oxides.

4. Discussion

The measured porosity (3.1%) of plasma sprayed coatings is almost in agreement with the findings of Chen et al. (Ref 19), Erickson et al. (Ref 20), Hidalgo et al. (Ref 13, 21), and Belzunce et al. (Ref 22), where the authors have reported porosity values varying from 0.8 to 4%. Microhardness plots indicated a little higher microhardness values of the substrate steels at the substrate bond coat interface perhaps caused by the high speed impact of coating particles (Ref 12, 13, 21). The microhardness values for the Ni-20Cr plasma sprayed coating are within the range of microhardness values reported for plasma sprayed coatings by Vuoristo et al. (Ref 23) and Chen and Hutchings (Ref 24).

A fragile scale with a tendency toward spalling has been observed for all the boiler steels used in the present investigation. The uncoated GrA1 steel showed severe spalling as can also be inferred from the weight gain plots since this steel has shown weight loss instead of weight gain due to spalling. Identical results have also been reported by Wang (Ref 3) in which severe scaling and spalling were observed for 2.25Cr-1Mo steel during 1000 h cyclic study at 740 °C in a medium-BTU coal fired boiler. Spalling of the scale to the extent of 70% was observed.

A comparatively milder attack for the uncoated T11 and T22 steels might be attributed to the presence of chromium in the inner scale, as identified by the EDAX analysis across the cross sections of T11 and T22 chromium containing steels. The result has further been supported by the finding of Sadique et al. (Ref 25), where the presence of chromium in the inner scale has also been observed. The degradation rates observed in the current study are lower than the corrosion rate reported for a T11 type of steel by Miller and Krause (Ref 26), who reported around 0.965 and 1.473 mm/month degradation rate for two steels containing 17-20 wt.% chromium at 649 °C.

The Ni-20Cr coating has shown good resistance to E-C in the given environment. The weight gain and corrosion rate values indicate the protective behavior of this Ni-20Cr coating. The degradation rate of Ni-20Cr coated T11 steel is at a minimum and is found to be about 64% of the same uncoated steel.

Formation of hematite (Fe_2O_3), as revealed by the x-ray diffractograms for uncoated steels, might be due to the reaction of iron with oxygen since iron is the main constituent of boiler steels. The formation of such a type of oxides has also been analyzed by Prakash et al. (Ref 5) and Srikanth et al. (Ref 27) during the failure analysis of superheater tubes caused by fireside corrosion. The formation of Al_2O_3 might be caused by the deposition of ash on the eroded-corroded steels. The absence of sulphide formation, as indicated by the XRD analysis, is further supported by the findings of Crossley et al. (Ref 28) They reported that the presence of fly ash particles rich in magnetite reduced the concentration of SO_3 in the boiler system fired by mechanical stokers. XRD results are further supported by the EDAX analysis.

The phases revealed by XRD diffractograms for Ni-20Cr coated steels are found to be in agreement with those reported by Longa-Nova et al. (Ref 29), Calvarin et al. (Ref 30), and Nickel et al. (Ref 31). The formation of Fe_2O_3 and Al_2O_3 might be due to diffusion from the substrate and bond coat and also to ash deposition. The presence of such phases in slag has also been reported by John (Ref 32) in his study on slag, gas, and deposit

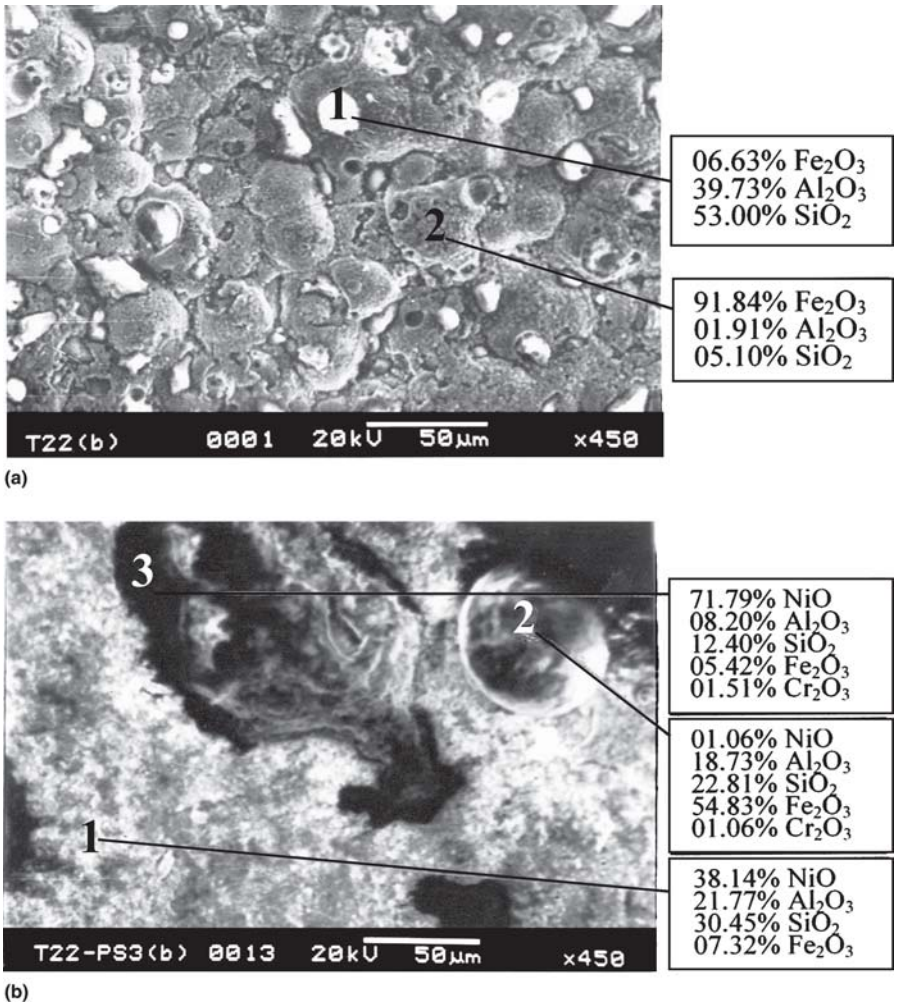

Fig. 5 Surface scale morphology and EDAX analysis for T22 boiler steel exposed to platen superheater of the coal fired boiler for 1000 h at 755 °C: (a) uncoated and (b) Ni-20 Cr coated

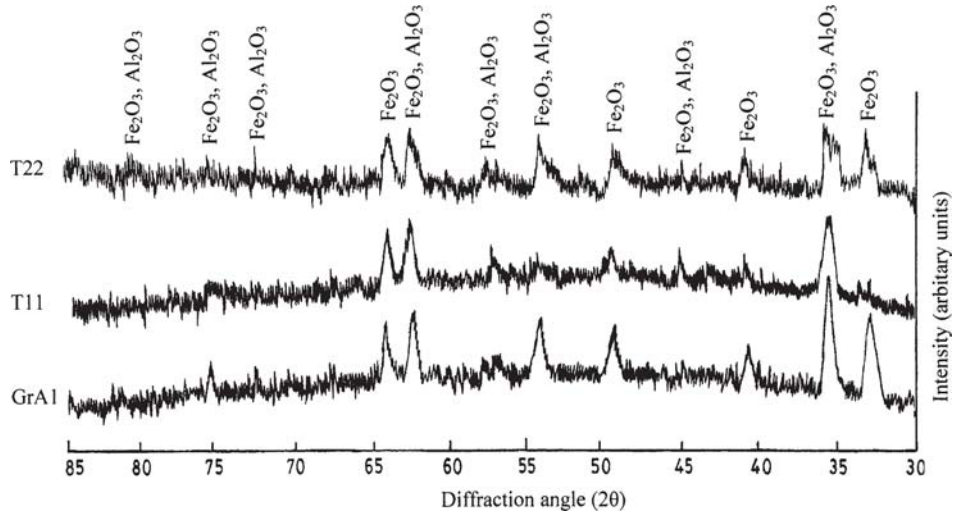

Fig. 6 XRD profiles for uncoated GrA1, T11, and T22 boiler steels exposed to platen superheater of the coal fired boiler for 1000 h at 755 °C

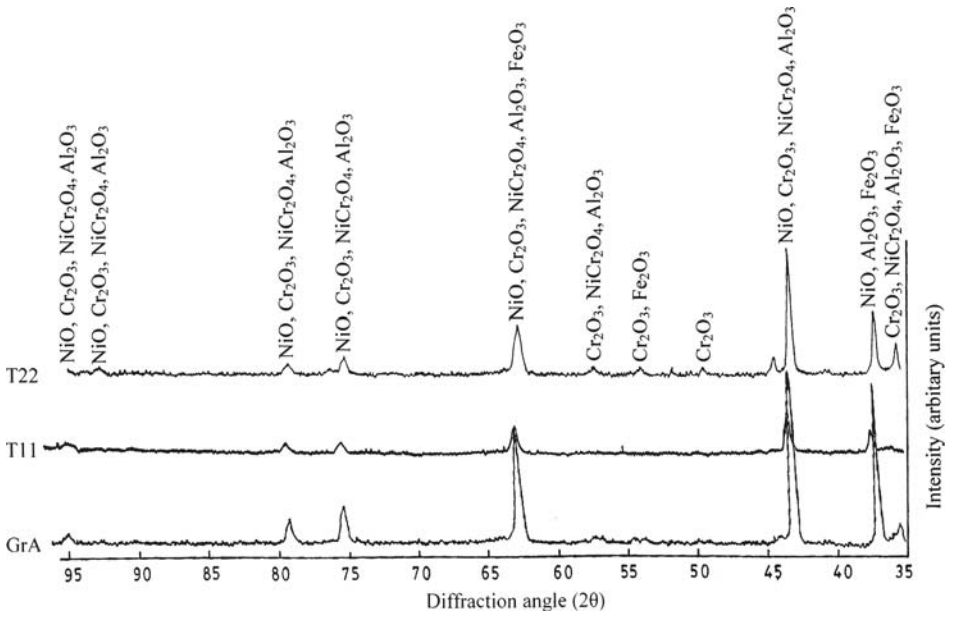

Fig. 7 XRD profiles for Ni-20Cr coated steels with bond coat exposed to platen superheater of the coal fired boiler for 1000 hours at 755 °C

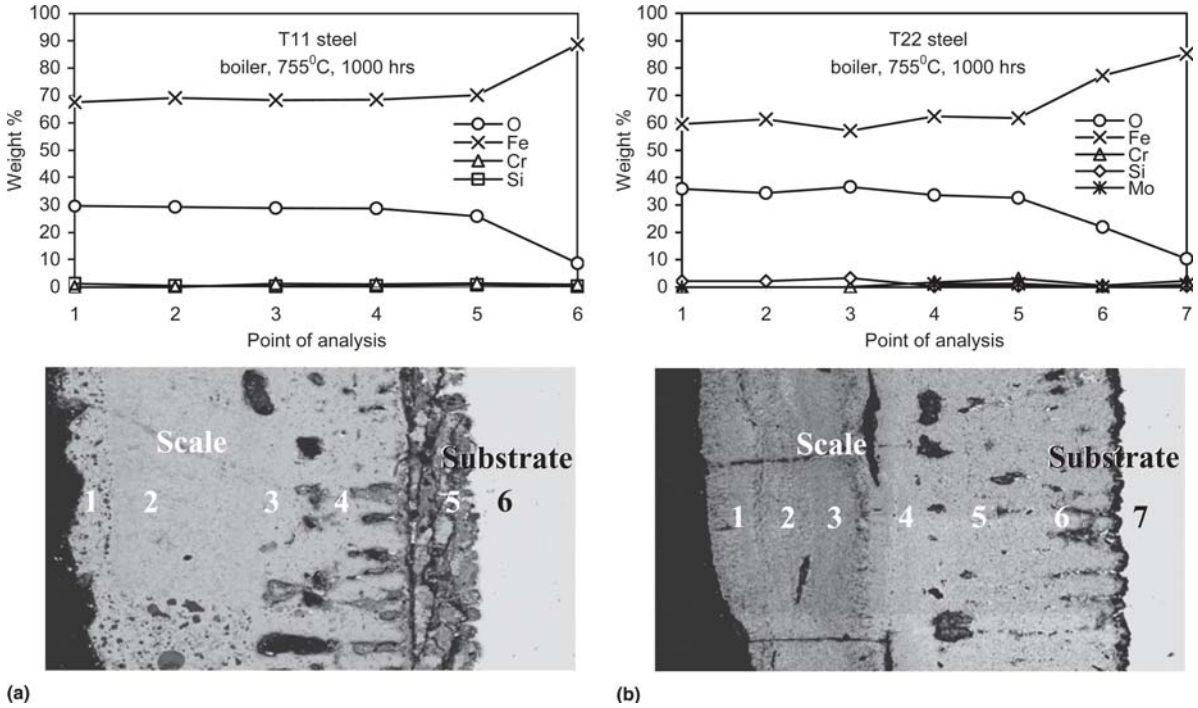

Fig. 8 Oxide scale morphology and elemental composition variation across the cross section of uncoated boiler steels exposed to platen superheater of the coal fired boiler for 1000 h at 755 °C: (a) T11, 90× and (b) T22, 70×

thermochemistry in a coal gasifier. The possibility for the formation of such a phase in the ash constituents during combustion has further been reported by Nelson et al. (Ref 33). EDAX and EPMA analysis further confirmed the formation of such phases alongside with indication of ash deposition.

The embedment of ash particles in the scale of uncoated boiler tube steels has been further confirmed by the EPMA analysis of the spalled scale piece of GrA1 steel. X-ray maps reveal the coexistence of aluminium and silicon, which indicate the presence of ash particles. Levy has also observed the presence of mixture of bed material constituents in the outer scale deposits during E-C of tubing steels in combustion boiler environments (Ref 4).

The cross-section EDAX analysis for GrA1, Ni-20Cr coated

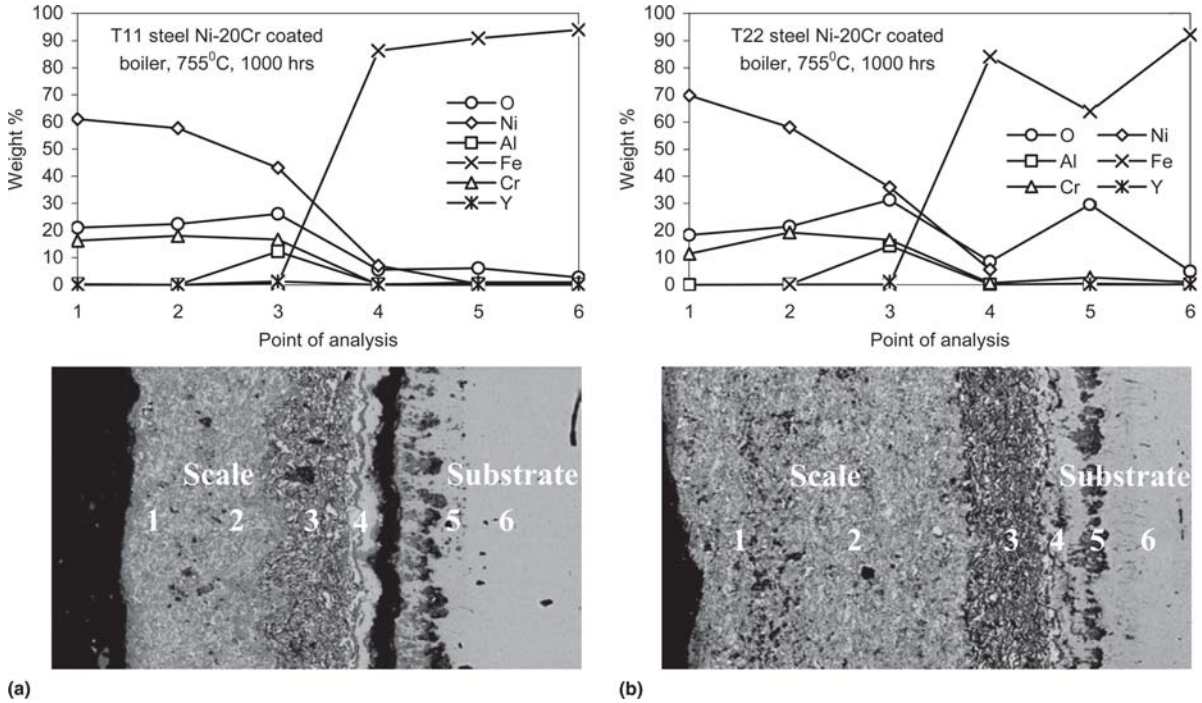

Fig. 9 Oxide scale morphology and elemental composition variation across the cross section of Ni-20Cr coating with bond coat exposed to platen superheater of the coal fired boiler for 1000 h at 755 °C having substrate steels (a) T11, 100×, and (b) T22, 90×

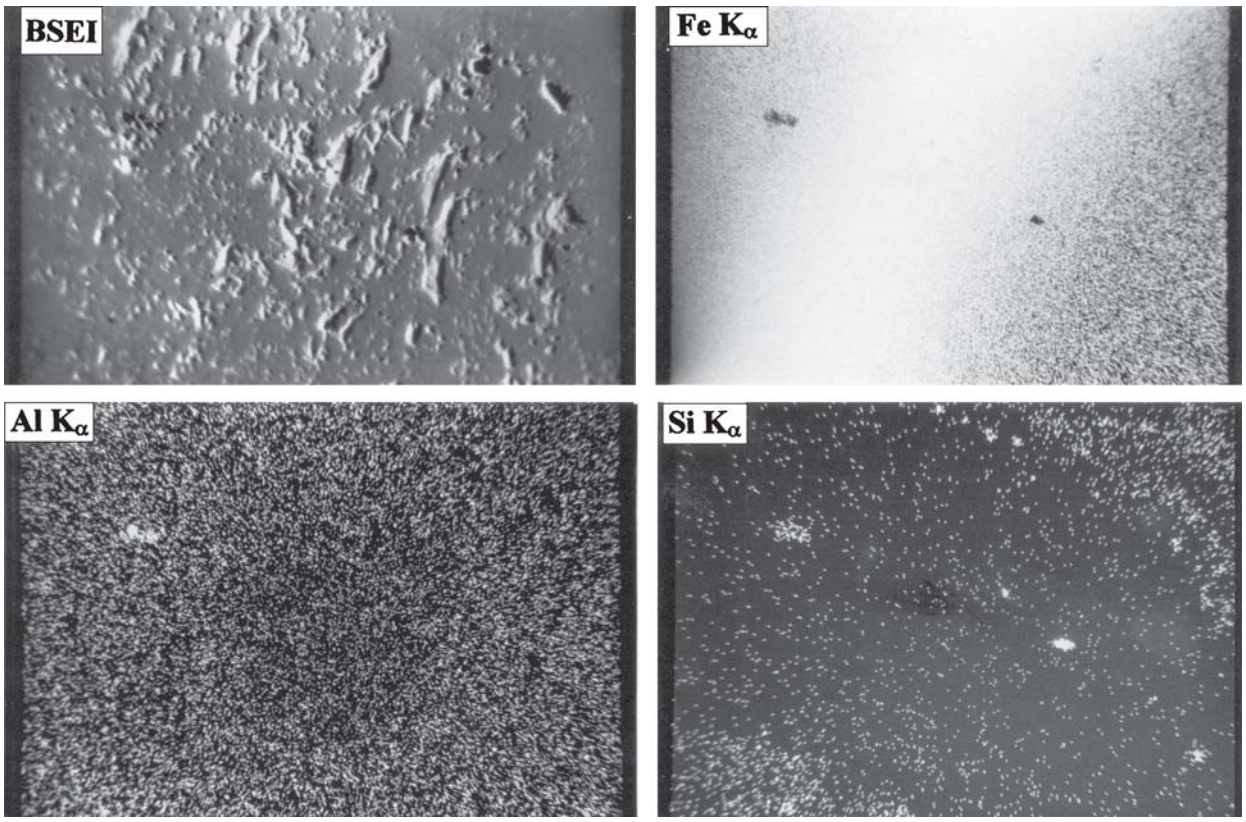

Fig. 10 BSEI and x-ray mapping of the spalled scale piece of GrA1 substrate steel exposed to platen superheater of the coal fired boiler for 1000 h at 755 °C

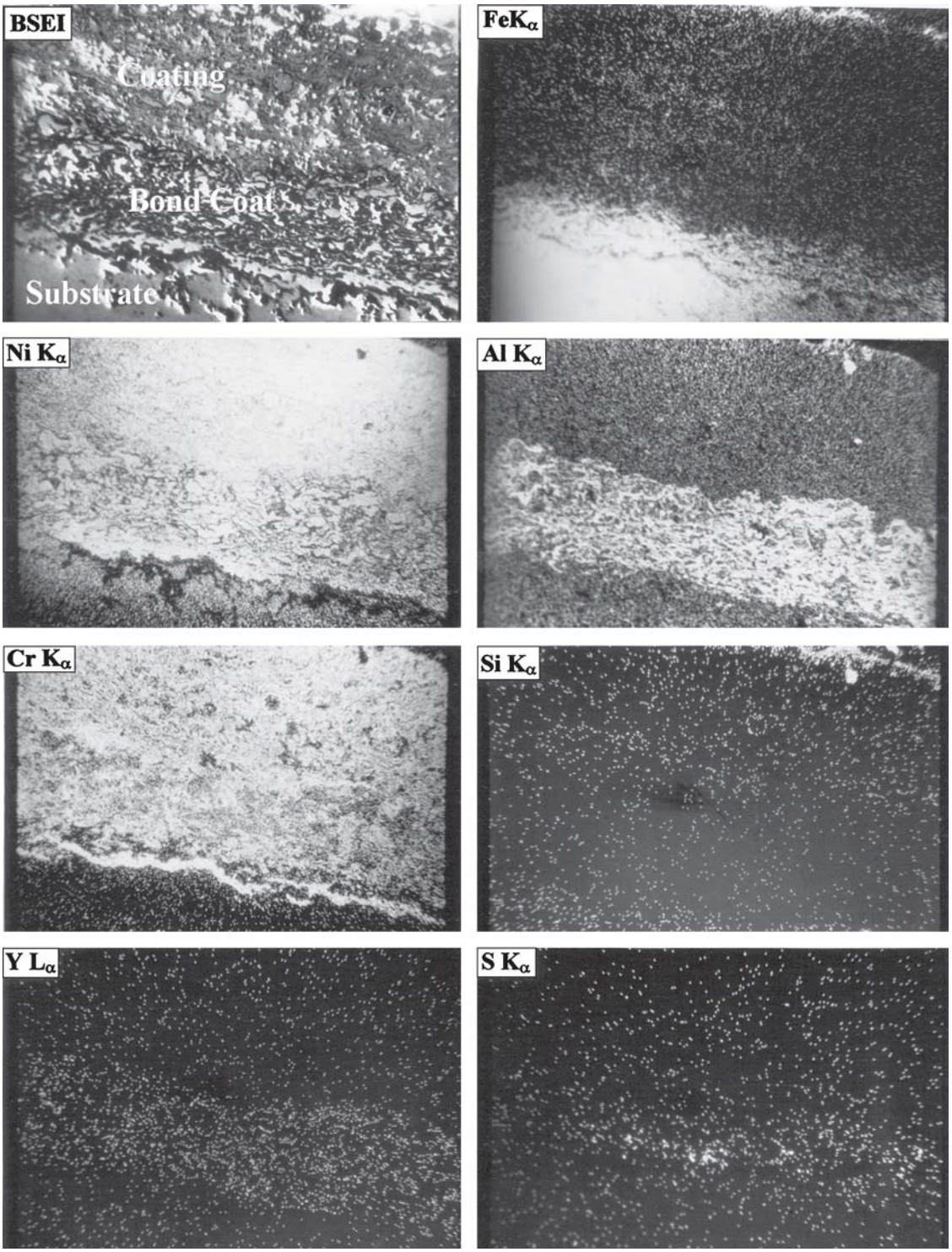

Fig. 11 BSEI and elemental x-ray mapping of the cross section of Ni-20Cr coated GrA1 steel with bond coat exposed to platen superheater of the coal fired boiler for 1000 h at 755 °C

steel shown in Fig. 9 indicates the outer layer of the scale to be rich in nickel. The diffusion of nickel to the outer scale to form NiO resulted in nickel depletion in the rest of the coating. The outward diffusion of nickel to form an outer scale leaves the coating depleted in nickel and richer in chromium to form an inner scale of chromium, as was also observed by Calvarin et al. (Ref 30). EPMA also confirms the formation of an outer NiO scale and inner scale of Cr_2O_3 (Fig. 11). The possible mechanism of attack for this coating is shown in Fig. 13. The top-most scale is rich in nickel, and then a chromium rich layer lying just above

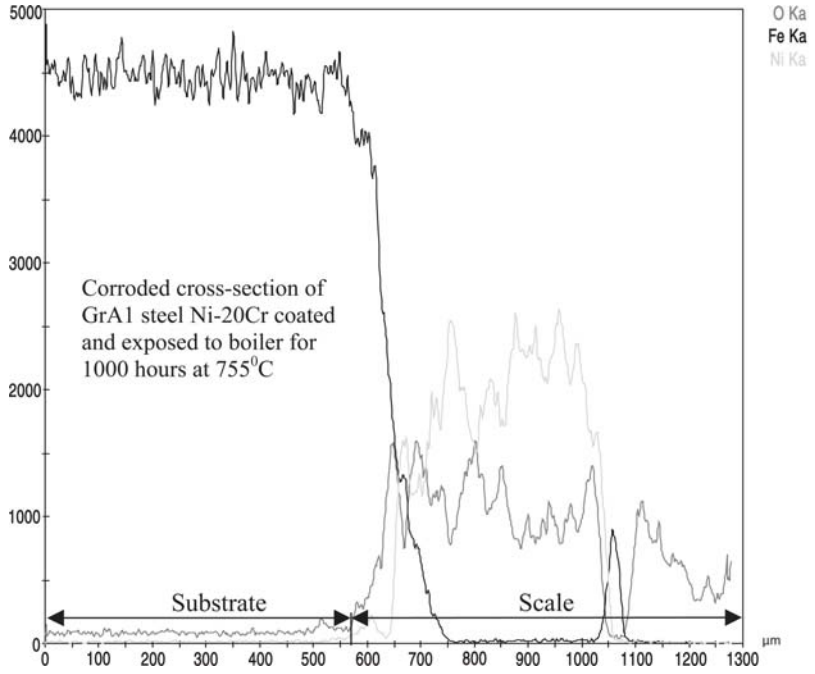

Fig. 12 EPMA elemental line profile analysis of the cross section of the GrA1 steel Ni-20Cr coated with bond coat exposed to platen superheater of the coal fired boiler for 1000 h at 755 °C

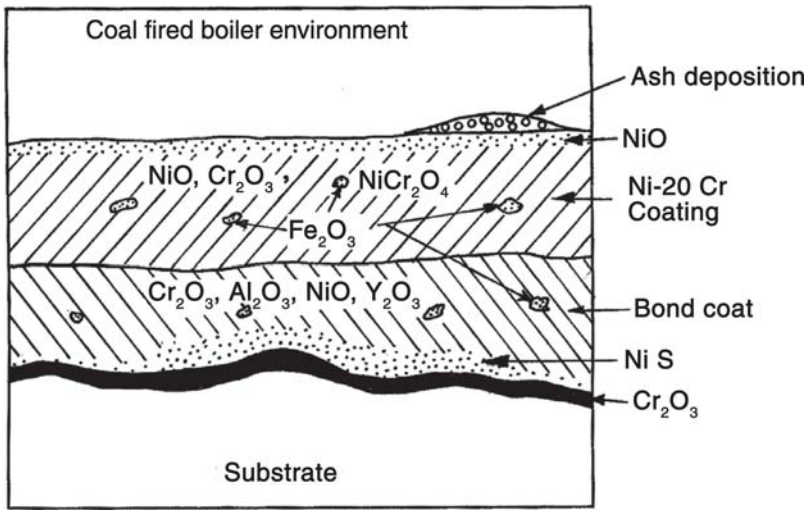

Fig. 13 Schematic diagram showing possible hot corrosion mechanisms for the Ni-20Cr coated GrA1 steel exposed to the coal fired boiler for 1000 hours at 755 °C

the bond coat is followed by an intermediate layer where nickel and chromium are coexisting, which confirms the formation of spinel. The continuous thin band of chromium lying at the bond coat-substrate interface blocks the transport of species to the substrate, which contributes to the protection of the base steels.

The mechanism of attack might be assumed to proceed identically to the oxidation of coatings because the presence of ash might have reduced the sulphur activities. The reaction mechanism for this Ni-20Cr coating might be as given below:

$$Ni + \frac{1}{2} O_2 \rightarrow NiO$$

The oxygen might have penetrated through this porous and loose structured layer of NiO (Ref 34) and reacted with chromium to form chromia:

$$2Cr + \frac{3}{2} O_2 \rightarrow Cr_2O_3$$

The outer interface of this inner chromia layer is richer in nickel, which might have led to the growth of spinel of nickel-chromium as per the reaction suggested by Calvarin et al. (Ref 30):

$$Cr_2O_3 + Ni + \frac{1}{2} O_2 \rightarrow NiCr_2O_4$$

5. Conclusions

The uncoated T22 steel showed better resistance to hot corrosion in boiler environment as compared with T11 and GrA1 bare steels. The inferior behavior of the uncoated GrA1 steel in boiler environment is perhaps due to the observed heavy spalling. All the plasma sprayed steels have shown better degradation resistance than uncoated steels. The minimum degradation rate was observed for T11 Ni-20Cr coated steel.

The embedment of ash particles has been observed in the uncoated and coated steels after exposure to boiler environment. The presence of ash has resulted in a decrease of the sulphur activities. Decreased sulphur activated lead only oxidation of uncoated and coated steels. The better E-C resistance of the Ni-20Cr plasma sprayed steels might be attributed to the observed presence of a continuous chromium rich layer just at the scale substrate interface, which blocks the transport of reacting species through it.

References

1. R.A. Rapp, J.H. Devan, D.L. Douglass, P.C. Nordine, F.S. Pettit, and D.P. Whittle, High Temperature Corrosion in Energy Systems, *Mater. Sci. Eng.,* 1981, 50, p 1-17
2. S. Danyluk and J.Y. Park, Technical Note: Corrosion and Grain Boundary Penetration in Type 316 Stainless Steel Exposed to a Coal Gasification Environment, *Corrosion,* 1979, 35 (12), p 575-576
3. D. Wang, Corrosion Behavior of Chromized and/or Aluminized 2¼Cr-1Mo Steel in Medium-BTU Coal Gasifier Environments, *Surf. Coat. Technol.,* 1988, 36, p 49-60
4. A.V. Levy, The Erosion-Corrosion of Tubing Steels in Combustion Boiler Environments, *Corros. Sci.,* 1993, 35 (5-8), p 1035-1043
5. S. Prakash, S. Singh, B.S. Sidhu, and A. Madeshia, Tube Failures in Coal Fired Boilers, S. Ray, S. Singh, and S.K. Nath, Ed., *Proc. National Seminar on Advances in Material and Processing,* IIT, R.K. Printers and Publishers, Roorkee, India, 2001, p 245-253
6. N. Priyantha, P. Jayaweera, A. Sanjurjo, K. Lau, F. Lu, and K. Krist, Corrosion-Resistant Metallic Coatings for Applications in Highly Aggressive Environments, *Surf. Coat. Technol.,* 163-64, p 31-36
7. M. Yoshiba, Effect of Hot Corrosion on the Mechanical Performances of Superalloys and Coating Systems, *Corros. Sci.,* 1993, 35 (5-8), p 1115-1124
8. P. Fauchais, J. F. Coudert, and M. Vardelle, Transient Phenomena in Plasma Torches and in Plasma Sprayed Coating Generation, *J. Phys. IV,* 1997, 7, p C4-187-198
9. R.F. Bunshah, *Handbook of Hard Coatings, Deposition Technologies, Properties and Applications,* Noyes Pub., Park Ridge, NJ, 2001
10. M.D. Modi, S.C. Modi, and M.M. Mayuram, A Case Study on the Use of Plasma Sprayed Oxide Ceramic Coatings in Hot Extrusion Dies for Non-Ferrous Metals, *Proc. 11th Int. Thermal Spraying Conf.,* September 8-12, Montreal, Canada, 1986, p 359-366
11. C. Wu and M. Okuyama, Evaluation of High Temperature Corrosion Resistance of Al Plasma Spray Coatings in Molten Sulfates at 1073 K by Electrochemical Measurements, *Mater. Trans., JIM,* 1996, 37 (5), p 991-997
12. V.H. Hidalgo, F.J.B. Varela, and E.F. Rico, Erosion Wear and Mechanical Properties of Plasma-Sprayed Nickel- and Iron-Based Coatings Subjected to Service Conditions in Boilers, *Trib. Int.,* 1997, 30 (9), p 641-649
13. V.H. Hidalgo, F.J.B. Varela, S.P. Martinez, and S.G. Espana, Characterization and High Temperature Behaviour of Cr_3C_2-NiCr Plasma Sprayed Coatings, *Proc. of the United Thermal Spray Conf.,* Germany, 1999, p 683-686
14. V.H. Hidalgo, J.B. Varela, J.M. Calle, and A.C. Menendez, Characterisation of NiCr Flame and Plasma Sprayed Coatings for Use in High Temperature Regions of Boilers, *Surf. Eng.,* 2000, 16 (2), p 137-142
15. B.S. Sidhu and S. Prakash, Evaluation of the Corrosion Behaviour of Plasma-Sprayed Ni_3Al Coatings on Steel in Oxidation and Molten Salt Environment at 900°C, *Surf. Coat. Technol.,* 2003, 166 (1), p 89-100
16. B. S. Sidhu and S. Prakash, Plasma Spray Coatings of Ni-20Cr on Boiler Tube Steel and Evaluation of Its Oxidation Behaviour at 900°C in Air, *J. Corros. Sci. Eng.,* 2003, 6, Paper 88.
17. B.S. Sidhu, D. Puri, and S. Prakash, Characterisations of Plasma Sprayed and Laser Remelted NiCrAlY Bond Coats and Ni_3Al Coatings on Boiler Tube Steels, *Mater. Sci. Eng. A,* 2004, 368 (1-2), p 149-158
18. B.S. Sidhu, D. Puri, and S. Prakash, Mechanical and Metallurgical Properties of Plasma Sprayed and Laser Remelted Ni-20Cr and Stellite-6 Coatings, *J. Mater. Process. Technol.,* 2005, 159 (3), p 347-355
19. H.C. Chen, Z.Y. Liu, and Y.C. Chuang, Degradation of Plasma-Sprayed Alumina and Zirconia Coatings on Stainless Steel During Thermal Cycling and Hot Corrosion, *Thin Solid Films,* 1993, 223 (1), p 56-64
20. L.C. Erickson, R. Westergard, U. Wiklund, N. Axen, H.M. Hawthorne, and S. Hogmark, Cohesion in Plasma-Sprayed Coatings: A Comparison Between Evaluation Methods, *Wear,* 1998, 214, p 30-37
21. V.H. Hidalgo, F.J.B. Varela, and A.C. Menendez, Characterization and High Temperature Behaviour of Thermal Sprayed Coatings Used in Boilers, *Proc. of the 15th Int. Thermal Spray Conf.,* May 25-29, Nice, France, 1998, p 617-621
22. F.J. Belzunce, V. Higuera, and S. Poveda, High Temperature Oxidation of HFPD Thermal-Sprayed MCrAlY Coatings, *Mater. Sci. Eng. A,* 2001, 297 (1-2), p 162-167
23. P. Vuoristo, K. Niemi, A. Makela, and T. Mantyla, Abrasion and Erosion Wear Resistance of Cr_3C_2-NiCr Coatings Prepared by Plasma, Detonation and High-Velocity Oxyfuel Spraying, *Proc. of the 7th National Thermal Spray Conf.,* Boston, MA, 1994, p 121-126
24. H. Chen and I.M. Hutchings, Abrasive Wear Resistance of Plasma-Sprayed Tungsten Carbide-Cobalt Coatings, *Surf. Coat. Technol.,* 1998, 107, p 106-114
25. S.E. Sadique, A.H. Mollah, M.S. Islam, M.M. Ali, M.H.H. Megat, and S. Basri, High-Temperature Oxidation Behavior of Iron-Chromium-Aluminum Alloys, *Oxid. Met.,* 2000, 54 (5-6), p 385-400
26. P.D. Miller and H.H. Krause, Factors Influencing the Corrosion of Boiler Steels in Municipal Incinerators, *Corrosion,* 1971, 27 (1), p 31-45
27. S. Srikanth, B. Ravikumar, S.K. Das, K. Gopalakrishna, K. Nandakumar, and P. Vijayan, Analysis of Failures in Boiler Tubes Due to Fireside Corrosion in a Waste Heat Recovery Boiler, *Eng. Failure Anal.,* 2003, 10, p 59-66
28. H.E. Crossley, A. Poll, and F. Sweett, The Reduction of Sulphur Trioxide by Constituents of Boiler Flue Dust, *J. Inst. Fuel,* 1948, 21, p 207-209
29. Y. Longa-Nava, Y.S. Zhang, M. Takemoto, and R.A. Rapp, Hot Corrosion of Nickel-Chromium and Nickel-Chromium-Aluminum Thermal-Spray Coatings by Sodium Sulfate-Sodium Metavanadate Salt, *Corrosion,* 1996, 52 (9), p 680-689
30. G. Calvarin, R. Molins, and A.M. Huntz, Oxidation Mechanism of Ni-20Cr Foils and Its Relation to the Oxide-Scale Microstructure, *Oxid. Met.,* 2000, 53 (1-2), p 25-48
31. H. Nickel, W.J. Quadakkers, and L. Singheiser, Analysis of Corrosion Layers on Protective Coatings and High Temperature Materials in Simulated Service Environments of Modern Power Plants Using SNMS, SIMS, SEM, TEM, RBS and X-Ray Diffraction Studies, *Anal. Bioanal. Chem.,* 2002, 374, p 581-587
32. R.C. John, Slag, Gas and Deposit Thermochemistry in a Coal Gasifier, *J. Electrochem. Soc.,* 1986, 133 (1), p 205-211
33. H.W. Nelson, H.H. Krause, E.W. Ungar, A.A. Putnam, C.J. Slunder, P.D. Miller, J.D. Hummel, and B.A. Landry, A Review of Available Information on Corrosion and Deposits in Coal- and Oil-Fired Boilers and Gas Turbines, *Report of ASME Research Committee on Corrosion and Deposits from Combustion Gases,* Pergamon Press and ASME, New York, 1959.
34. X. Wu, D. Weng, Z. Chen, and L. Xu, Effects of Plasma-Sprayed NiCrAl/ZrO_2 Intermediate on the Combination Ability of Coatings, *Surf. Coat. Technol.,* 2001, 140, p 231-237